

# Investigation of Adsorption and Desorption Characteristics of Metal-Organic Frameworks for The Development of Desalination Systems

Riaz, Nadia

Laboratory for Energy and Env. Engineering Research, Department of Agricultural Engineering

Sultan, Muhammad

Laboratory for Energy and Env. Engineering Research, Department of Agricultural Engineering

<https://doi.org/10.5109/4739231>

---

出版情報 : Proceedings of International Exchange and Innovation Conference on Engineering & Sciences (IEICES). 7, pp.261-267, 2021-10-21. Interdisciplinary Graduate School of Engineering Sciences, Kyushu University

バージョン :

権利関係 :



# Investigation of Adsorption and Desorption Characteristics of Metal-Organic Frameworks for The Development of Desalination Systems

Nadia Riaz<sup>1</sup>, Muhammad Sultan<sup>1\*</sup>

<sup>1</sup>Laboratory for Energy and Env. Engineering Research, Department of Agricultural Engineering, Bahauddin Zakariya University, Multan 60800, Pakistan

\*Corresponding author email: muhammadsultan@bzu.edu.pk; sultan@kyudai.jp

**Abstract:** An increased lack of access to potable fresh water and sanitation has been witnessed in recent years and is damaging communities, particularly in underprivileged countries. Innovative nanostructured materials are essential to reducing the separation process's capital & operational costs and energy intensity. Metal-organic frameworks (MOFs) are emerging and promising adsorbents with notable attributes such as easy uptake and release of water at moderate temperatures and low relative pressures, along with improved working capacities. This study is focused on the characteristics and potential applications of MOFs in water desalination. According to the results, desalination covers a wide range of inflection points which is  $0.15 < \alpha < 0.5$ . The MOFs falling in this range (ideal for desalination) are Al-fumarate and MIL-101(Cr). Finally, the adsorption uptake capacities are evaluated for further development depending on their suitability for desalination systems.

**Keywords:** Metal-organic frameworks (MOFs); adsorption/desorption; adsorption characteristics; desalination, adsorption desalination.

## 1. INTRODUCTION

Around seven hundred million people worldwide suffer from water scarcity. By 2025, 1.8 billion people will be living in places with absolute water shortages [1]. Unfortunately, this scenario is projected to become worse. In order to alleviate the water shortage and related water contamination issues, desalination techniques have provided an innovative alternative in the recent decade. The common methods employed for water desalination include humidification - dehumidification desalination (HDH), multiple-effect distillation (MED), solar distillation (SD), multi-stage flash distillation (MSF), and vapor compression distillation (MVC), including technologies such as nanofiltration (NF), electro-dialysis (ED), reverse osmosis (RO) and forward osmosis (FO). Some of the significant advantages of desalination systems include utilizing waste heat, reduced maintenance cost, reduced electricity utilization, and cogeneration ability with cooling and freshwater production. However, owing to the significant emissions from current desalination processes and their impact on global warming - advanced systems with reduced energy utilization and CO<sub>2</sub> emissions are required. Therefore, various researchers have made investigations to improve the conventional desalination methods. Consequently, the adsorption desalination (AD) technique has recently gained colossal consideration and interest due to its significant benefits and low evaporation temperature, lowering the fouling effect [2]. A brief comparison of various desalination technologies is presented in Table 1. Researchers evaluated the AD systems, as shown in Error! Reference source not found.. Scheele (1774) and Fontana (1777) reported the adsorption phenomena [3], and de Saussure observed that heat developed during the cycle, and the porosity of the solid material was the principal cause of adsorption. Since then, adsorption has proliferated in numerous investigative studies [4]. Various researches are conducted to analyze the performance of adsorbent-adsorbate pairs employed in the desalination systems. The typical commercially accepted adsorbents are silica gel, zeolites, activated carbon, and zeolite-like materials [5]. In addition, recent researches have thoroughly evaluated the employment of

metallic-organic frameworks (MOFs) for water treatment and gas separation.

MOFs' distinct porous structures, added with various secondary building units (SBUs), chemical functions, high-specific surfaces, and particle structures, make them more preferable to conventional materials [6]. In addition, the MOF-integrated membranes show improved material compatibility with rigid frameworks, which often cause membrane porosity and segregation to block [7]. Water stability is one of the essential characteristics of MOFs used in water treatment [8]. These can function as nanofillers that can be integrated into membranes of some specific types. Therefore, MOFs can be produced in their pure state, and their synthesis has made them more stable materials.

Table 1. An overview of desalination technology's GHG emissions and energy use.

	Electric al energy consum ption (kWh m <sup>-3</sup> )	Thermal energy consump tion (kWh m <sup>-3</sup> )	CO <sub>2</sub> emiss ions (kg m <sup>-3</sup> )	Cost (\$ m <sup>-3</sup> )	Ref .
<b>MSF</b>	69.44– 83.33	69.44– 83.33	20.4– 25.0	1.07	[9]
<b>MED</b>	1.5–5	41.67– 61.11	11.8– 17.6	0.83	[9]
<b>RO</b>	4–8	0	2.79	0.76	[10] [11]
<b>Adso rptio n</b>	1.38	39.8	11.2	0.3	[12]

This paper investigates and provides an update on the MOFs' adsorption/desorption characteristics and stability in liquid systems. First, the study constructed a database of 383 MOF samples reported in the literature to evaluate their water adsorption properties. Then, according to the criteria, a suite of 18 MOFs is recognized for selective specific applications. By utilizing this water adsorption database of MOFs, the

adsorption and desorption isotherms are replotted to evaluate and compare systematically. Based on this study, It was shown that the MOF structure and hydrophilicity or hydrophobicity of the building blocks are responsible for the adsorption isotherm shapes, hysteresis, steepness, step location, and leading adsorption. Finally, the analysis defines the characteristics and potential of various MOFs for practical applications in desalination, chillers, heat pumps, water harvesting, and air conditioning systems.

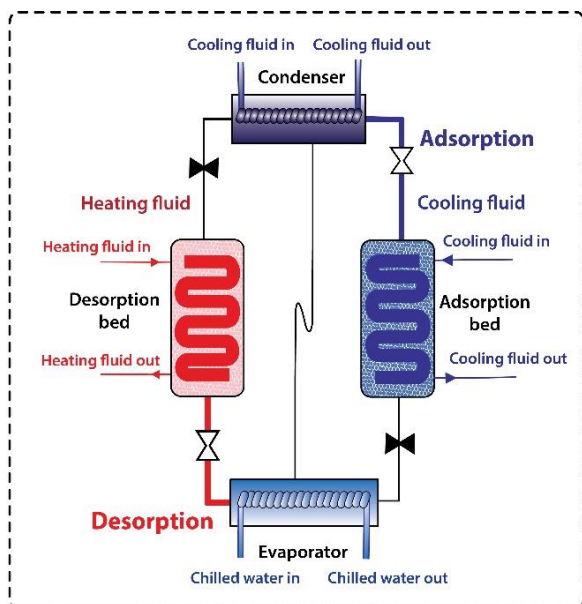


Fig. 1 Conventional adsorption system.

Most MOF applications are still in a phase of exploration. For these applications, the design features of systems and conceptual process designs are therefore taken as a precedent for further R&D against current adsorbents.

## 2. METHODOLOGY

The water adsorption isotherms of MOFs were initially collected from the literature. The water adsorption features of 383 MOF samples were assessed systematically in this work, based on the six criteria, which resulted in 18 kinds of MOFs (shown in Table 2), which meet the requirements mentioned below. Appropriate MOFs for water adsorption uses have been described by following six criteria [13]:

1. Hydrothermal stability
2. A steep uptake isotherm at a specific relative pressure for condensation or pore-filling
3. an ample water working capacity for the requisite maximum delivery of water or energy effect
4. Minimal or no hysteresis in desorption (indoor humidity control is an exception)
5. High cycling durability
6. Facile adsorption-desorption, heat kinetics, and fast mass for the desired energy efficiency.

The chosen MOFs were first to be assessed. The isotherms of the chosen MOF were then traced for water adsorption/desorption, based on published data as shown in Fig. 2 and Fig. 3. The isotherms are in the units of volume-specific ( $\text{g}/\text{cm}^3$  MOF) as they are common in the application by specifying the sample volume being occupied for a specific water capacity. The relative pressure and temperature dependence for water uptake W

( $p/p_0, T$ ) may be easily represented after Polanyi [14] and Dubinin [15], which defines an adsorbent potential ( $p/p_0, T$ ) in equation (i) and equation (ii). The connection between Dubinin-Astakhov is commonly used, with all isotherms breaking down to a single feature curve with a step at MOF-specific adsorbent characteristic energy,  $E$ .

$$W\left(\frac{p}{p_0}, T\right) \Rightarrow W(A) \quad (i)$$

$$= W_{\max} \exp \left[ -\left( \frac{A}{E} \right)^n \right]$$

$$A = -RT \ln \left( \frac{p}{p_0} \right) \quad (ii)$$

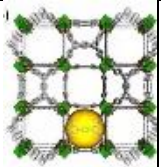
Similarly, the water adsorption/desorption properties and mechanism of some of these 18 selected MOFs are presented further based on the types of metal valencies, linkers, and the type of adsorption mechanism. Finally, the classification of some of the adsorption isotherms is made based on the IUPAC definition [16].


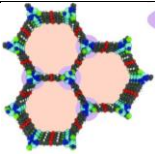
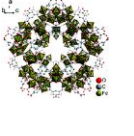
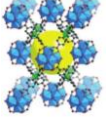

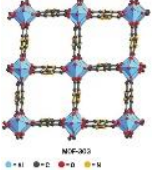
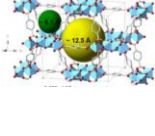
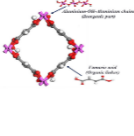
### a. Water Adsorption process

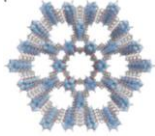
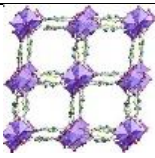
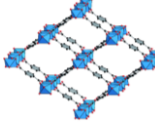
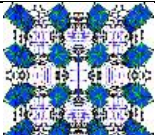
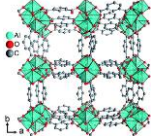
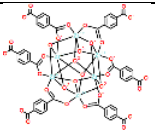
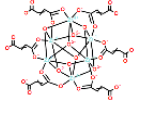
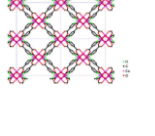
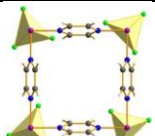
The water adsorption applications comprise a comparable construction with two interconnected essential components, a water processing unit, and a water-MOF contactor, having a cyclic manner of operation. Since Chang's presented a study in 2006, water adsorption characteristics in MOFs are widely investigated [17]. Water cluster adsorption is widespread in the formation of layers since most investigated. Aromatic hydrophobic linkers are part of MOFs. On hydrophilic sites in MOFs, water clusters can be formed after water nucleation. The open and closed systems can be differentiated as - "closed" systems that exchange energy with the environment or surroundings, and "open" systems are those which also supply or remove water along with the exchange of energy with the surroundings [18]. The type and efficiency of application are determined by precise connection and operational methods and conditions. Power density and productivity are crucial to the reallocation of heat, while water collection, rate, and productivity are sought.

The dependence on partial temperature and pressure in both subunits directs the functioning of the water vapor-liquid phase interaction, recorded on psychrometric charts. The inclusion of MOF in the water-MOF contactor changes these properties through sorption. In addition, water and energy transit must also be accounted for in all applications [19].

Table 2. Crystalline structure and physical properties of the identified MOFs.

Material	$\alpha$ [—] <sup>1</sup>	$q_{\max}$ [ $\text{g}/\text{g}$ ] <sup>1</sup>	$V_p$ [ $\text{cm}^3/\text{g}$ ]	Stability	Crystalline structure	Ref.
Cr-soc-MOF-1	0.69	1.95	2.1	No loss in $\Delta q$ over 100 adsorption cycles/with signific		[20]

				ant hysteresis		
MI L- 101 (Cr)	0.4	1.73	-	-		[2122]
Co <sub>2</sub> Cl <sub>2</sub> (BTD)	0.29	0.97	-	6.3% loss in $\Delta q$ over 30 adsorption cycles		[23]
MI L- 100 (Fe)	0.35	0.79	0.82	-		[24]
M OF- 841 (Zr)	0.22	0.51	0.53	7% loss in $q_{max}$ after 5 adsorption cycles		[25]
Y- shp- M OF- 5	0.63	0.48	0.63	9% loss in $q_{max}$ after 1000 adsorption cycles /with significant hysteresis		[26]
M OF- 303 (Al)	0.13	0.45	0.54	No loss in $q_{max}$ over 5 adsorption cycles		[4]
MI L- 125 (Ti)- NH <sub>2</sub>	0.2	0.45	0.51	-		[27]
Al- fu- mar- ate	0.27	0.45	0.48	No loss in $\Delta q$ over 4500 adsorption cycles		[28]

MI P- 200 (Zr)	0.18	0.45	0.40	6% loss in $\Delta q$ over 1-10 adsorption cycles and no loss in $\Delta q$ over 10-40 adsorption cycles		[29]
CA U- 23(Al)	0.27	0.42	0.48	No loss in $\Delta q$ over 5000 adsorption cycles		[30]
MI L- 53(Al)- OH	0.75	0.40	-	-		[31]
MI L- 160 (Al)	0.09	0.38	0.40	No loss in $\Delta q$ over 10 adsorption cycles		[32]
CA U- 10(Al)- H	0.16	0.37	-	No loss in $\Delta q$ over 9 adsorption cycles		[33]
Ui O- 66( Zr)	0.31	0.37	0.35	No loss in $q_{max}$ over 2 adsorption cycles		[34]
M OF- 801 (Zr)	0.09	0.36	0.45	Stable over 5 adsorption cycles		[25]
Co- CU K-1	0.12	0.30	0.26	No loss in $\Delta q$ over 50 adsorption cycles		[35]
AI FFI VE- 1- Ni	0.02	0.24	0.1	No loss in $\Delta q$ over 14 adsorption cycles		[36]



### 3. RESULTS AND DISCUSSION

The physical properties of 383 MOFs were assessed at specific operational conditions provided in the literature. The 18 MOFs were found to be in accordance with the criteria defined for their suitability and application in water adsorption systems.

#### 3.1 Chemisorption on Open Metal Sites

The UiO-66(Zr) [34] framework or zirconium is linked by BDC linkers having an eight-coordinated structure after dehydration is converted into a seven-coordinated face-centered cubic lattice. A triangular aperture of a diameter of 0.6 nm links the tetrahedral cavity with a diameter of around 0.9 nm and the octahedral cavity having a diameter of around 1.1 nm. The DFT computation with pair distribution function, PXRD, neutron powder diffraction, and EXAFS analysis was employed to witness the structural transformation of UiO-66(Zr). Surprisingly, the SBU's ability to chemisorb water is entirely reversible.

#### 3.2 Capillary Condensation

Capillary condensation and cluster adsorption precede the adsorption of water in pores greater than the critical diameter  $D_c$ . As the adsorption branch is unable to attain the thermodynamic equilibrium, a hysteresis loop is observed among the adsorption-desorption branches. An equation for  $D_c$  calculation is presented as:

$$D_c = \frac{4\sigma T_c}{T_c - T} \quad (\text{iii})$$

where  $\sigma$ ,  $T_c$ , and  $T$  are the Van der Waals diameter of water, critical temperature, and actual temperature for which the values are 0.28nm, 647 K, and room temperature, respectively. Therefore, the critical diameter is found to be about 2.0 nm. Hence, it is predicted that the pores having  $D_c$  greater than 2.0 nm presents adsorption-desorption hysteresis and capillary condensation behavior.

MIL-101(Cr) [21][22] comprises two mesoporous cages in the ratio of 2:1, having 2.9 and 3.4 nm as internal free diameters, respectively. MIL-101(Cr) has a high water capacity because of its high framework porosity. Furthermore, its high hydrothermal stability ensures significant cycling durability. Due to this reason, the MOF has numerous applications in the adsorption of water [24]. The MIL-101(Cr)'s adsorption isotherm exhibits two separate steps, as shown in Fig. 2. First, the cluster growth and water nucleation are caused at a  $p/p_0 = 0.39$  relative pressure, when initially low uptake is witnessed. On unsaturated metal sites, the 80 kJ mol<sup>-1</sup> (high) heat of adsorption represents the probability of chemisorption. The smaller cage's pore filling occurs at  $p/p_0 = 0.39$ , which is the first steep step and the pore filling of the larger cage occurs at  $p/p_0 = 0.44$ , which is the second round. A maximum number of water molecules are physisorbed, validated by the fact that in both of the steps, the heat of adsorption was closer to evaporation enthalpy. A solid hysteresis loop can be fully described as capillary condensation that occurs in mesoporous cages.

MIL-100 (Cr) and MIL-101(Cr) have the same MTN zeotype architecture but have different linkers. In MIL-100(Fe), as the iron takes the place of chromium, water adsorption behavior is significantly affected, as iron is

not damaging to humans [37]. Therefore, MIL-100(Fe) encompasses those isotherms that have shapes identical to MIL-101(Cr), having a lower inflection point and a lower capacity (Fig. 2). Without the loss of capacity, 2000 adsorption cycles were carried out, showing their outstanding endurance [38].

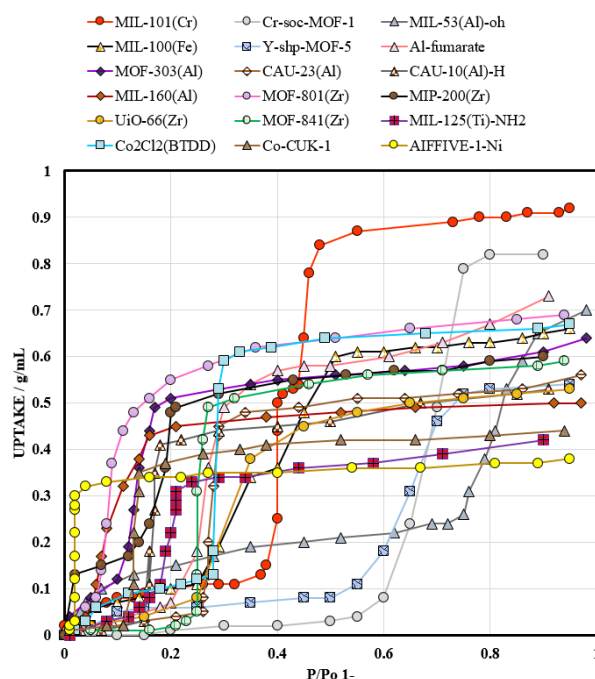


Fig. 2 Water adsorption isotherms of M(III)-carboxylate MOFs, M(IV)-carboxylate and M(II)-azolate. Samples and data used for MOF-841(Zr)[25], MIL-100(Fe)[24], MIL-53(Al)-OH [31], Y-shp-MOF-5[26], Cr-soc-MOF-1 [20], Co<sub>2</sub>Cl<sub>2</sub>(BTDD)[23], Al-fumarate[28], CAU-10(Al)-H [33], MIL-160(Al)(@303K)[32], MOF-303(Al) [4], UiO-66(Zr)[34], MOF-801(Zr)[25], MIP-200(Zr)(@303 K)[29], MIL-101(Cr)[21][22], MIL-125(Ti)-NH<sub>2</sub>[27], AIFIVE-1-Ni (@308 K)[36], and Co-CUK-1 (@303 K)[35], CAU-23(Al)[30].

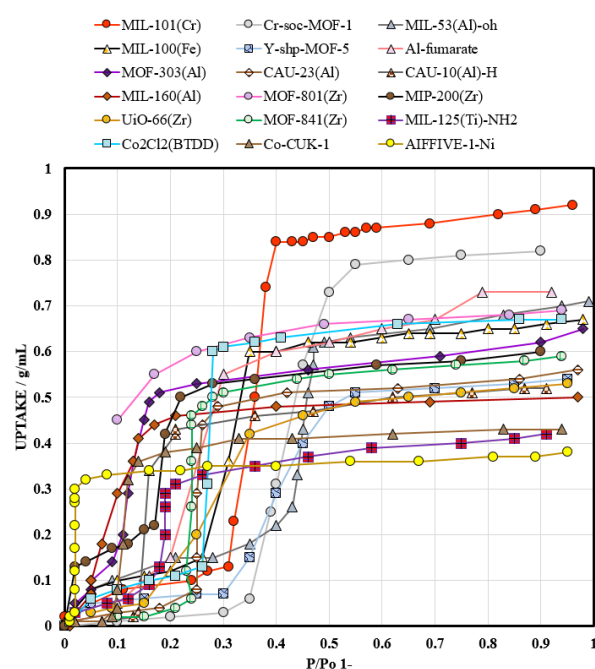


Fig. 3 Water desorption isotherms of M(III)-carboxylate MOFs, M(IV)-carboxylate and M(II)-azolate. Samples

and data used for MOF-841(Zr)[25], MIL-100(Fe)[24], MIL-53(Al)-OH [31], Y-shp-MOF-5[26], Cr-soc-MOF-1 [20],  $\text{Co}_2\text{Cl}_2$ (BTDD)[23], Al-fumarate[28], CAU-10(Al)-H [33], MIL-160(Al)(@303K)[32], MOF-303(Al) [4], UiO-66(Zr)[34], MOF-801(Zr)[25], MIP-200(Zr)(@303 K)[29], MIL-101(Cr)[21][22], MIL-125(Ti)- $\text{NH}_2$ [27], AIFIVE-1-Ni (@308 K)[36], and Co- CUK-1 (@303 K)[35], CAU-23(Al)[30].

### 3.3 Cluster Adsorption

Infinite rod-like SBUs connected by the 1D channels of BDC linkers are used in MIL-53. It exhibits a significant water-molecular breathing effect, as demonstrated by MIL-53(Al)-OH [31]. In the original MIL-53(Al) of its small pore structure, only a single water molecule is adsorbed in every metal unit at saturated vapor pressure. The addition of OH groups in the BDC linkers simplifies, and it becomes feasible to breathe at relatively high pressure, about  $p/p_0 = 0.75$ .

Pore-filling takes place at the big pore stage (free dimensions) MIL-53(Al)-OH metal units adsorb five water molecules. The structure restores at a desorption branch pressure of  $p/p_0 = 0.47$  to a thin pores phase (free size 1.9 nm 0.8 nm), leaving a significant hysteresis loop attributable to the breathing behavior (Fig. 2). As a result, the water adsorption exhibits a type V S-shaped isotherm (Fig. 2).

The CAU-10(Al)-H contains rod-like SBUs cis coupled to squared, sinusoidal channels of approximately 0.7 nm in diameter by 1, 3-BDC connectors. The material displays a favorable S-shaped adsorption isotherm with the  $p/p_0 = 0.16$  without hysteresis and significant lift. The rod-like SBUs of the CAU-23(Al)[30] are coordinated along the b-axis, with hydrophilic TDC linkers to create 1D square-shaped channels (length side of 0.76 nm). The SBUs consist of four successive trans-units (as noted in series MIL-53) and  $\text{AlO}_6$  polyhedra cis-corner sharing, as witnessed in the CAU-10(Al)-H series. The analysis shows an S-shaped isotherm with a steep  $p/p_0 = 0.27$  uptake. The water adsorption of MOF-303(Al) displays a type IV isotherm with a reduced inflection point at  $\alpha = 0.13$  and a rise starting at  $p/p_0 = 0.3$  [4] and undergoes a small hysteresis, moderate constant isosteric heat of adsorption, and high durability, shown by 150 repeatable adsorption cycles. The Y-shp-MOF-5195 structure shows an S-shaped, type-IV-like adsorption and desorption isotherms.

In MOF-801(Zr) [25], the amount of adsorbed water efficiently rises along with the pressure up to  $p/p_0 = 0.05$ , and at  $p/p_0 = 0.9$ , a final capacity of 0.36 g/g is reached Fig. 2. The water adsorption isotherm of MIP-200 (Zr)[29] has two regions with nearly no hysteresis on the desorption branch beyond  $p/p_0 = 0.05$  (Fig. 2). MOF-841(Zr) and MIL-125(Ti)- $\text{NH}_2$  exhibit type V water adsorption isotherm, where the latter has an s-shape. In MOF-841, there is a steep increase in the adsorption at  $p/p_0 = 0.2$  and starts to become flat at  $p/p_0 = 0.3$ , having a final capacity of around 0.5 g/g Fig. 2. In MIL-125(Ti)- $\text{NH}_2$ , the steep loading occurs at a reduced relative pressure  $p/p_0 = 0.2$ , and there is no desorption hysteresis.  $\text{Co}_2\text{Cl}_2$  (BTDD) exhibits 1D mesoporous channels having water uptake and release in the absence of hysteresis because of capillary condensation. The MOF shows a significant and steep step of uptake at  $p/p_0 = 0.29$ , Fig. 2 [23]. The water adsorption of AIFIVE-1-

Ni (KAUST-8)[36] is 0.22 g/g having type I isotherm, at a much decreased relative pressure ( $p/p_0 = 0.05$ ), Fig. 2. For its unique adsorption and regeneration characteristics, the usage of MOFs is significant here. CPO-27(Ni) may also be used to operate a one-bed system with evaporation, condenser, and desorption temperature of 40 °C, 5 °C, and 95 °C, respectively. The potential for a MOF was emphasized in the AD [40] with a single-bed system. The utility of MOFs for AD was shown by comparative research using CPO-27(Ni), Al-fumarate, and MIL-101(Cr). SDWP values were correspondingly 4.6, 6.3 and 11  $\text{m}^3/\text{tonne}$  MOF day at 20°, 25° and 25°C evaporation-adsorption condenser temperatures and high temperature for regeneration, i.e., 150°C. While this was the most significant mass density for MIL-101, 232, it demonstrates al-fumarate differs by ~40% per unit volume sorbent. Lower temperatures in regeneration below 70°C had little influence on their SDWP, while the performance of other MOFs had a considerable influence due to MIL-101 desorption hysteresis (Fig. 3) and the solid CPO-27 adsorption. Hysteresis of al-fumarate is scarcely evident and may consequently be regenerated at low temperatures. Subsequent research by the same team of two-bedded systems has verified that silica and CPO-27(Ni) has been removed in the function of the operating temperatures and operating mode. The water exhibits a high distilled quality, the lowest thermal and electrical consumption (SDWP up to 14  $\text{m}^3/\text{tonne}$  MOF day), and the lowest price of water (0.3 \$/ $\text{m}^3$ ) compared with other standard processes (multi-effect distillation, multistage flash, and reverse osmosis)[9]. The performance observed for adsorption desalination is excellent than those for the harvesting of water. This is mainly due to the broader range of humidity in AD and the technical development. These results demonstrate MOF's potential for adsorption desalination. In addition, the step position in the MOF isotherm and lack of hysteresis dictate the system operating range of temperatures. Although not a wide range of MOFs have yet been investigated, the reduced regeneration temperature shown for al-fumarate is particularly appealing.

### 4. CONCLUSION

This study revealed that out of 18 MOFs under consideration, 12 exhibits a 1D pore system having a 0.7 nm pore size. Most 1D MOFs exhibit a regular ordering. Moreover, the MOF improvement by linker functionalization with hydrophobic groups moves the step to higher relative pressures, and with hydrophilic groups, moves the step to lower. It is observed that even the change of metal from Co or Ni to Mg in CUK-1 raises hydrophobicity, shifting the step from  $p/p_0 = 0.12$  to 0.25. The results have shown that the MOFs evaluated in the study can be employed for various applications.

From the adsorption/desorption isotherms, a classification of MOFs is performed on the inflection points in the isotherm steps. Desalination covers a wide range of inflection points which is  $0.15 < \alpha < 0.5$ . The MOFs falling in this range (ideal for desalination) are MIL-101(Cr) and Al-fumarate. Similarly, very low inflection points ( $\alpha < 0.05$ ) cover AIFIVE-1-Ni, which can be used for desiccation. A range of  $0.1 < \alpha < 0.3$  includes Al-fumarate, CAU-23(Al), MOF-303(Al),

MOF-841(Zr), MIL-125(Ti)-NH, Co-CUK-1, CAU-10AD-H, MIL-160(Al), MOF-801(Zr),  $\text{Co}_2\text{Cl}_2$ (BTDD) for water harvesting and in heat pumps. For humidity control, Y-shp-MOF-5 and Cr-soc-MOF-1 can be employed. Al-fumarate barely shows hysteresis and can consequently be regenerated at reduced temperatures (as shown in Fig. 2 and Fig. 3). Productivities indicated for AD production are an order of magnitude more than those reported for water harvesting. The research analyses the possibility of MOFs in adsorption desalination. Isotherm position and absence of hysteresis influence operating temperatures. Al-fumarate is one of the few MOFs that have been investigated for such usage, but its reported low regeneration temperature is very promising for an energy-efficient operation. The step placement determines the system operating temperature window in MOF isotherm and by the absence of hysteresis. Although not many MOFs for this purpose have been investigated, Al-fumarate's proven low regeneration temperature is particularly promising for energy-efficient operation.

## 5. REFERENCES

- [1] H. Kummer, G. Földner, and S. K. Henninger, "Versatile siloxane based adsorbent coatings for fast water adsorption processes in thermally driven chillers and heat pumps," *Appl. Therm. Eng.*, vol. 85, pp. 1–8, 2015, doi: 10.1016/j.applthermaleng.2015.03.042.
- [2] E. Elsayed, R. Al-dadah, S. Mahmoud, P. A. Anderson, A. Elsayed, and P. G. Youssef, "CPO-27 (Ni), aluminium fumarate and MIL-101 (Cr) MOF materials for adsorption water desalination," *DES*, vol. 27, 2016, doi: 10.1016/j.desal.2016.07.030.
- [3] A. Dabrowski, "Adsorption - from theory to practice," *Adv. Colloid Interface Sci.*, vol. 93, pp. 135–224, 2001.
- [4] F. Fathieh, M. J. Kalmutzki, E. A. Kapustin, P. J. Waller, J. Yang, and O. M. Yaghi, "Practical water production from desert air," *Sci. Adv.*, pp. 1–10, 2018.
- [5] S. ULKU, "ADSORPTION HEAT PUMPS," *Heat Recover. Syst.*, vol. 6, pp. 277–284, 1986.
- [6] Y. R. He, Y. P. Tang, and D. Ma, "UiO-66 incorporated thin-film nanocomposite membranes for efficient selenium and arsenic removal," *J. Memb. Sci.*, 2017, doi: 10.1016/j.memsci.2017.06.061.
- [7] M. Kadhom, W. Hu, and B. Deng, "Thin Film Nanocomposite Membrane Filled with Metal-Organic Frameworks UiO-66 and MIL-125 Nanoparticles for Water Desalination," 2017, doi: 10.3390/membranes7020031.
- [8] C. Wang, X. Liu, K. Demir, J. Paul, and K. Li, "Applications of water stable metal-organic frameworks," *Chem. Soc. Rev.*, 2016, doi: 10.1039/C6CS00362A.
- [9] E. Elsayed, R. Al-dadah, S. Mahmoud, P. Anderson, and A. Elsayed, "Experimental testing of aluminium fumarate MOF for adsorption desalination," *Desalination*, vol. 475, no. October 2019, p. 114170, 2020, doi: 10.1016/j.desal.2019.114170.
- [10] Toufic Mezher, H. Fath, Z. Abbas, and A. Khaled, "Techno-economic assessment and environmental impacts of desalination technologies," *Desalination*, vol. 266, pp. 263–273, 2011, doi: 10.1016/j.desal.2010.08.035.
- [11] V. G. Gude, "Desalination and Sustainability – An Appraisal and Current Perspective," *Water Res.*, 2015, doi: 10.1016/j.watres.2015.11.012.
- [12] K. Choon, K. Thu, Y. Kim, A. Chakraborty, and G. Amy, "Adsorption desalination : An emerging low-cost thermal desalination method," *Desalination*, vol. 308, pp. 161–179, 2013, doi: 10.1016/j.desal.2012.07.030.
- [13] M. F. De Lange *et al.*, "Metal–Organic Frameworks in Adsorption-Driven Heat Pumps: The Potential of Alcohols as Working Fluids," 2015, doi: 10.1021/acs.langmuir.5b03272.
- [14] C. Wang, "Section III.—Theories of the adsorption of gases. A general survey and some additional remarks. Introductory paper to section III," *Trans. Faraday Soc.*, 1930.
- [15] W. Energetically and N. Surfaces, "The Potential Theory of Adsorption of Gases and Vapors for Adsorbents with Energetically Nonuniform Surfaces," *Chem. Rev.*, no. 13, 1969.
- [16] M. Thommes *et al.*, "Physisorption of gases, with special reference to the evaluation of surface area and pore size distribution (IUPAC Technical Report)," *Pure Appl. Chem.*, vol. 87, no. 9–10, pp. 1051–1069, 2015, doi: 10.1515/pac-2014-1117.
- [17] K. Hwang *et al.*, "Porous organic-inorganic hybrid materials and adsorbent comprising the same," 2012.
- [18] S. V. Id *et al.*, "Adsorption Heat Storage: State-of-the-Art and Future Perspectives," *Nanomaterials*, vol. 8, p. 522, 2018, doi: 10.3390/nano8070522.
- [19] A. Kodama, T. Hirayama, M. Goto, and T. Hirose, "The use of psychrometric charts for the optimisation of a thermal swing desiccant wheel," *Appl. Therm. Eng.*, vol. 21, pp. 1657–1674, 2001.
- [20] S. T. Abtab *et al.*, "Reticular Chemistry in Action: A Hydrolytically Stable MOF Capturing Twice Its Weight in Adsorbed Water," *Chem*, pp. 94–105, 2018, doi: 10.1016/j.chempr.2017.11.005.
- [21] M. F. De Lange, K. J. F. M. Verouden, T. J. H. Vlugt, J. Gascon, and F. Kapteijn, "Adsorption-Driven Heat Pumps: The Potential of Metal–Organic Frameworks," *Chem. Rev.*, 2020, doi: 10.1021/acs.chemrev.5b00059.
- [22] M. F. De Lange, S. Hamad, T. J. H. Vlugt, J. Gascon, and F. Kapteijn, "Understanding Adsorption of Highly Polar Vapors on Mesoporous MIL-100(Cr) and MIL-101(Cr): Experiments and Molecular Simulations," *J. Phys. Chem.*, vol. 100, no. Iii, 2013.
- [23] A. J. Rieth, S. Yang, E. N. Wang, and M. Dinca, "Record Atmospheric Fresh Water Capture and Heat Transfer with a Material Operating at the Water Uptake Reversibility Limit," *ACS Cent. Sci.*, 2017, doi: 10.1021/acscentsci.7b00186.
- [24] P. Küsgens *et al.*, "Characterization of metal-organic frameworks by water adsorption," *Microporous Mesoporous Mater.*, vol. 120, no. 3, pp. 325–330, 2009, doi:



- 10.1016/j.micromeso.2008.11.020.
- [25] H. Furukawa, F. Ga, M. R. Hudson, and O. M. Yaghi, "Water Adsorption in Porous Metal–Organic Frameworks and Related Materials," *J. Am. Chem. Soc.*, 2014.
- [26] R. G. Abdulhalim *et al.*, "A Fine-Tuned Metal–Organic Framework for Autonomous Indoor Moisture Control," *J. Am. Chem. Soc.*, 2017, doi: 10.1021/jacs.7b04132.
- [27] J. Bonnefoy, A. Legrand, B. Coasne, and D. Farrusseng, "Structure – property relationships of water adsorption in metal – organic frameworks," *New J. Chem.*, pp. 3102–3111, 2014, doi: 10.1039/c4nj00076e.
- [28] F. Jeremias, C. Janiak, and S. K. Henninger, "Advancement of sorption-based heat transformation by a metal coating of highly-stable, hydrophilic aluminium fumarate MOF," *R. Soc. Chem.*, pp. 24073–24082, 2014, doi: 10.1039/c4ra03794d.
- [29] S. Wang *et al.*, "A robust large-pore zirconium carboxylate metal–organic framework for energy-efficient water-sorption-driven refrigeration," *Nat. Energy*, 2000, doi: 10.1038/s41560-018-0261-6.
- [30] D. Lenzen *et al.*, "A metal–organic framework for efficient water-based ultra-low-temperature-driven cooling," *Nat. Commun.*, no. 2019, pp. 1–9, doi: 10.1038/s41467-019-10960-0.
- [31] A. Shigematsu, T. Yamada, and H. Kitagawa, "Wide Control of Proton Conductivity in Porous Coordination Polymers," *J. Am. Chem. Soc.*, pp. 2034–2036, 2011.
- [32] A. Cadiau *et al.*, "Design of Hydrophilic Metal Organic Framework Water Adsorbents for Heat Reallocation," *Adv. Mater.*, pp. 4775–4780, 2015, doi: 10.1002/adma.201502418.
- [33] M. F. De Lange and F. Kapteijn, "Manufacture of dense CAU-10-H coatings for application in adsorption driven heat pumps: optimization and characterization," *R. Soc. Chem.*, vol. 17, no. 31, 2015, doi: 10.1039/c5ce00789e.
- [34] A. D. Wiersum *et al.*, "An Evaluation of UiO-66 for Gas-Based Applications," *Chem. - Asian J.*, vol. 6, no. 12, pp. 3270–3280, 2011, doi: 10.1002/asia.201100201.
- [35] J. S. Lee *et al.*, "Porous Metal–Organic Framework CUK-1 for Adsorption Heat Allocation toward Green Applications of Natural Refrigerant Water," *Appl. Mater. Interfaces*, 2019, doi: 10.1021/acsami.9b02605.
- [36] A. Cadiau *et al.*, "Hydrolytically stable fluorinated metal-organic frameworks for energy-efficient dehydration," *Science (80-. )*, vol. 735, no. May, pp. 731–735, 2017.
- [37] P. G. M. Mileo, K. H. Cho, J. Park, J. Chang, and G. Maurin, "Unraveling the Water Adsorption Mechanism in the Mesoporous MIL-100(Fe) Metal–Organic Framework," vol. 100, 2019, doi: 10.1021/acs.jpcc.9b06228.
- [38] G. Ak, R. Matsuda, and K. Susumu, "Highly Porous and Stable Coordination Polymers as Water Sorption Materials," *Chem. Soc. Japan*, vol. 293, no. 5, pp. 360–361, 2010, doi: 10.1246/cl.2010.360.
- [39] E. Article and O. K. Farha, "Water stabilization of Zr6-based metal–organic frameworks via solvent-assisted ligand incorporation," *Chem. Sci.*, vol. 00, pp. 1–5, 2015, doi: 10.1039/C5SC01784J.
- [40] P. George, "Experimental investigation of adsorption water desalination / cooling system using CPO-27Ni MOF Experimental Investigation of Adsorption Water Desalination / Cooling System Using CPO - 27Ni MOF," 2021, doi: 10.1016/j.desal.2016.11.008.